

2021 SCEC Project Report

UCSB BROADBAND KINEMATIC RUPTURE SIMULATION WITH A DOUBLE CORNER SOURCE SPECTRUM

Principal Investigators: **Ralph Archuleta and Chen Ji**
Earth Research Institute
University of California, Santa Barbara

Abstract

We continue our efforts to understand the earthquake source spectra and subsequently improve our ability to predict ground motion for future earthquakes. First, when computing broadband ground motion using the UCSB method, we explicitly specify a source spectrum for its moment rate function. During our recent modification, we assume the target source spectra is JA19_2S, inferred from our study of the NGA West-2 dataset (Ji and Archuleta, 2020). After testing it with BBP events, we identify two modifications for the scaling relations. Second, the “*stress parameter*” (hereinafter referred to it as $\widetilde{\Delta\sigma}$) (Boore, 1983) is used during stochastic ground motion simulations but the physical meaning of $\widetilde{\Delta\sigma}$ has not been clearly defined. We conducted a review of a collection of theoretical source spectral models (Ji *et al.*, 2022). We find despite the well-known variation in predicting static stress drop $\Delta\sigma_s$ from the seismic moment and corner frequency, all models, especially three conventional models, suggest that earthquakes radiate about half of the available strain energy into the surrounding medium. This suggests not only a robust method to estimate stress drop using source spectra but also a physical interpretation to $\widetilde{\Delta\sigma}$. We infer that the constancy of the “*stress parameter*” ($\widetilde{\Delta\sigma}$) found in engineering seismology (Boore, 1983; Atkinson and Beresnev, 1998) is similar to having constant apparent stress, σ_a (e.g., Ide and Beroza, 2001).

Intellectual Merit

The earthquake source spectra count important information about earthquake rupture. Most published stress estimates, especially for moderate and small earthquakes, are inferred from the corner frequency of source spectra. However, the stress estimates are model dependent. The intellectual merits of our works include c) two new modifications when we apply the DCF source spectral models to constrain the realistic rupture realization. b) a robust method for stress drop estimation; c) a clear physical mean of “*stress parameter*” ($\widetilde{\Delta\sigma}$).

Broader Impacts

A critical need for earthquake engineering is knowledge of near-source ground motion from damaging crustal earthquakes. While the data are becoming more plentiful (e.g., Ancheta *et al.*, 2014), there is a notable lack of data within 20 km of the causative fault for earthquakes with $M > 6$. Physics-based kinematic earthquake scenarios can provide computed broadband accelerograms for a wide range of magnitudes and distances.

Proposed tasks

In this study, we attempted to refine the scaling relations when using double corner frequency source spectral model JA19_2S (Ji and Archuleta, 2020) to constrain the source realization of future earthquakes.

Results

We had asked two questions. 1) During the BBP simulations, we assume the spectrum of the moment rate functions of realistic rupture models can be treated as the average source spectrum of an earthquake. What are the necessary adjustments caused by this assumption? 2) what is the physical mean of the “*stress parameter*” (hereinafter referred to it as $\widetilde{\Delta\sigma}$) (Boore, 1983) that has been used extensively during stochastic ground motion simulations?

1. Revised Scaling relations of BBP simulations

We recently revised the UCSB method (Liu *et al.*, 2006; Schmedes *et al.*, 2013; Crempien and Archuleta, 2015) recently under the support of SCEC. For a given earthquake, we require that the spectrum of its cumulative moment rate function obeys double corner frequency (DCF) spectral model JA19_2S (Ji and Archuleta, 2020),

$$\Omega_0(f, f_{c1}, f_{c2}) = \frac{M_0}{\left[1 + \left(\frac{f}{f_{c1}}\right)^4\right]^{1/4} \left[1 + \left(\frac{f}{f_{c2}}\right)^4\right]^{1/4}} \quad (1)$$

with two corner frequencies (f_{c1} & f_{c2}) that follow the scaling relations,

$$\begin{aligned} \log(f_{c1}(M)) &= \begin{cases} 1.474 - 0.415M & M < 5.3 \\ 2.375 - 0.585M & M \geq 5.3 \end{cases} \text{ \& } \\ \log(f_{c2}(M)) &= 3.250 - 0.5M \end{aligned} \quad (2)$$

Here M_0 denotes the seismic moment and M is the moment magnitude (Hanks and Kanamori, 1979). Figure 1 shows an acceleration spectrum predicted using the JA19_2S model for an Mw 5.3 earthquake with $f_{c1} = 0.19 \text{ Hz}$ and $f_{c2} = 4 \text{ Hz}$. The empirical conversions $T_d = 1/\pi f_{c1}$ (T_d is the total rupture duration) and $\bar{T}_R = 0.8/f_{c2}$ (\bar{T}_R is the average rise time) were proposed (Ji and Archuleta, 2020).

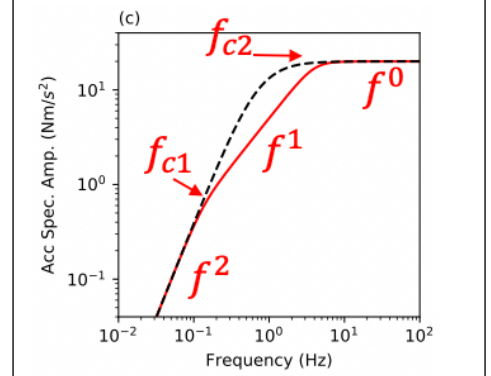


Figure 1. An example DCF acceleration spectrum (red line). The dashed line is single corner Brune's spectrum which shares the same low- and high- frequency asymptotes.

We benchmarked this method with the earthquakes on the SCEC broadband platform (BBP). We find that data are very sensitive to f_{c1} and f_{c2} . For most BBP earthquakes, using f_{c1} and f_{c2} directly predicted by JA19_2S cannot guarantee satisfactory fits to 5%-damped pseudo-absolute-acceleration spectra (PSA). Additional event-based adjustments to these two corner frequencies are required. This motivates us to investigate whether BBP earthquakes are consistent with known source scaling relations.

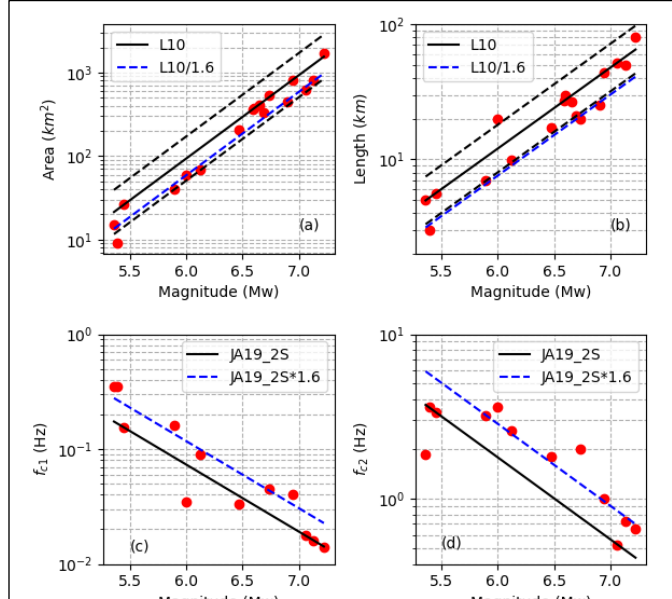


Figure 2. Comparison of source parameters (red dots) used by BBP simulations, L10 (Leonard, 2010) and JA19_2S (Ji and Archuleta, 2020). The black dashed lines in (a) and (b) indicate $\pm 1\sigma$ uncertainty. Note, the four Japan earthquakes have not been included in c & d.

Figure 2 shows the comparisons of rupture area (A) and rupture length (L), f_{c1} and f_{c2} of BBP earthquakes, spanning a magnitude range from 5.36 to 7.2. Note that A and L are currently default fault parameters used by all BBP modelers. Leonard (2010) re-analyzed multiple published data sets and proposed a set of self-consistent scaling relations between seismic moment (M_0), rupture area (A), rupture length (L) and rupture width (W), which are referred to as **L10** model. Leonard (2010) found that $\log(A) \sim Mw - 4.03$ fault scaling applies for all shallow crustal earthquakes, which suggests an average static stress drop $\Delta\sigma_s$ of 3.0 MPa. As shown in Figure 1a, the **L10** relation marks the upper bound of the rupture areas for these BBP events. The fault

areas of about half of BBP earthquakes are about 1.6 times smaller than **L10** predictions. A smaller fault area implies a larger static stress drop. The corresponding $\Delta\sigma_s$ for these earthquakes is 6.0 MPa. The 2008 Mw 5.4 Chino Hill earthquake is an outlier. It has a fault area of 9 km², suggesting an abnormally high static stress drop $\Delta\sigma_s$ of 14 MPa. This result is consistent with the previous finite fault study (Shao *et al.*, 2012). For a comparison, Leonard (2010) found that the mean $\Delta\sigma_s$ of earthquakes in stable continental regions (SCR) is 5.8 MPa.

Leonard (2010) found that for $Mw > \sim 5$ earthquakes, fault length (L) and width (W) scale with the seismic moment as $M_0 \propto L^{2.5}$ and $W \propto L^{2/3}$. The former can be rewritten as $\log(L) = 0.6Mw - 2.5$, which is in good agreement with the rupture length L for $\sim 55\%$ of BBP earthquakes (including three $Mw > 7$ earthquakes). But another $\sim 40\%$ of BBP earthquakes feature fault lengths 1.6 times smaller than the **L10** model (blue dashed line, Figure 2b). On the other hand, the 2004 Mw 6 Parkfield earthquake is an outlier with a significantly longer fault length (20 km) than the prediction of the **L10** model (Figure 2b). In Figures 2c and 2d, we compare the optimal values of f_{c1} and f_{c2} with the predictions of JA19_2S. Note that only California BBP events are included. For f_{c1} , we again see an interesting bimodal distribution. The optimal f_{c1} values of about half of BBP earthquakes (including the three $M > 7$ earthquakes) are consistent with JA19_2S, while the values for another half of earthquakes are 1.6 times larger. For f_{c2} , however, most optimal values of BBP earthquakes are 1.6 times larger than predicted by the JA19_2S model.

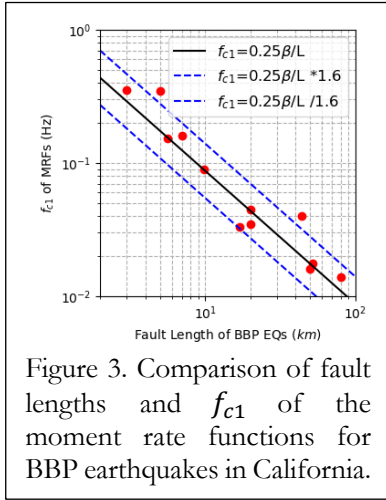


Figure 3. Comparison of fault lengths and f_{c1} of the moment rate functions for BBP earthquakes in California.

Ji and Archuleta (2022) found that the non-self-similar f_{c1} scaling relation of JA19_2S and the fault length scaling relation of the **L10** model can be reconciled if the apparent rupture velocity (\tilde{V}_r , defined as L/T_d , L and T_d are fault length and rupture duration, respectively) is 0.8β , here β denotes the S wave speed at the source. It leads to a relation $f_{c1} \sim 0.25\beta/L$. As shown in Figure 3, this relation matches the f_{c1} of the optimal DCF moment rate functions better than JA19_2S (Figure 2c). Hence the deviations from the **L10** model and the JA19_2S are correlated. $f_{c1} \sim 0.25\beta/L$ should be used when the fault length L is available. We are still investigating the scatters of f_{c2} values relative to JA19_2S but use it as an empirical correction. It is noteworthy that f_{c1} and f_{c2} of JA19_2S are associated with the mean source spectra of the earthquakes with a given magnitude. During the BBP simulations, f_{c1} and f_{c2} are

associated with the moment rate functions of realistic rupture models. Although in the literature, the spectrum of moment rate function and the average source spectral model are often used interchangeably, our results suggest they might be different systematically.

2. The physical meaning of “stress parameter”

Boore (1983) introduced the terminology “stress parameter” ($\tilde{\Delta\sigma}$), following the seminal work of Hanks and McGuire (1981). For a given earthquake, he used $\tilde{\Delta\sigma}$, seismic moment M_0 , and the k value of Brune’s model to predict the corner frequency of its source spectrum. This source spectrum was subsequently used to predict PGA, PGV, local magnitude, and response spectra successfully. $\tilde{\Delta\sigma}$ has ever since been widely used as a key source parameter during the stochastic strong ground motion simulations (e.g., Atkinson and Boore, 1995; Atkinson and Silva, 1997; Boore, 2003; Graves and Pitarka, 2010; Boore *et al.*, 2014). However, the physical meaning of the stress parameter $\tilde{\Delta\sigma}$ has not

been clearly defined. The discrepancy between values of $\widetilde{\Delta\sigma}$ and average static stress drop $\Delta\sigma_s$ has been reported (e.g., Hanks and McGuire, 1981; Boore, 1983). It led Atkinson and Beresnev (1998) to a well-known letter entitled “*don’t call it stress drop*”, in which they argued that $\widetilde{\Delta\sigma}$ may bear no relationship to real stresses on the fault surface.

Table 1. Comparisons of dynamic circular crack and slip pulse models^a (Modified from Ji et al., 2022)

Parameters	Brune Model	Madariaga Model	K&S model	W&D models		
				EC ^c	GP ^c	SS ^c
$V_R (\times \beta)$	∞	0.9	0.9	0.84-0.88	0.81-0.85	0.74-0.78
k (S wave)	0.372	0.21	0.26	0.27	0.36	0.31
$(k)^{-3}/19.425$	1.0	5.56	2.93	2.62	1.10	1.73
η_R	0.466 ^b	0.533	0.48	0.40	0.65	0.46
$\Delta\sigma_s$ (if $\sigma_a=1$ MPa)	4.29	3.75	4.17	5.0	2.35 (3.08) ^d	3.13 (4.35) ^d

^a K&S: Kaneko and Shearer (2014, 2015); W&D: Wang and Day (2017).

^b Brune model only considered the S wave radiation (Brune, 1970).

^c EC: expanding crack, GP: growing pulse, SS: steady state pulse (Wang and Day, 2017).

^d Value inside the parentheses is the estimate by further assuming $\Delta\sigma_s^E = \Delta\sigma_s$

Because of the challenge in determining rupture area A , most published estimates of average static stress drop $\Delta\sigma_s$, particularly for small and even moderate magnitude earthquakes, have been made using observed source spectra following the seminal work of Brune (1970). The result we especially refer to as $\Delta\sigma_{f_c}$: $\Delta\sigma_{f_c}$ is proportional to f_c^3/k^3 , where f_c denotes corner frequency and k is a model dependent constant. The relation between $\Delta\sigma_{f_c}$ and $\Delta\sigma_s$ is then subject to cubed uncertainty from not only the measurement error of f_c but also the model uncertainty of k (Ji et al., 2022). Ji et al. (2022) recently reviewed several published source spectral models. They found that regardless of the well-known large discrepancy among the crack models (of 5.56) in $\Delta\sigma_s$ for a given $(M_0 - f_c)$ pair (the fourth row of Table 1), these theoretical models estimate similar seismic radiation efficiency η_R (ratio of seismic radiated energy E_R and the available strain energy ΔW (e.g., Hussein and Randall, 1976; Venkataraman and Kanamori, 2004)) (Table 1, the fifth row). It implies that to estimate $\Delta\sigma_s$ through apparent stress σ_a is a more robust approach (Ji et al., 2022).

Ji et al. (2022) emphasized that during the forward stochastic strong ground motion simulations with Brune’s ω^{-2} source spectra and Brune’s k , the analytical relation $\widetilde{\Delta\sigma}/\sigma_a = 2/\eta_R \sim 4.3$ (Andrews, 1986; Singh and Ordaz, 1994) firmly holds. In principle, $\widetilde{\Delta\sigma}$ is simply another form of apparent stress σ_a . The mean σ_a of Mw>5.5 shallow crustal earthquakes was found to be about ~ 1.0 MPa, independent of magnitude (Ide and Beroza, 2001; Ide et al., 2003; Prieto et al., 2004; Baltay et al., 2011; Convers and Newman, 2011; Kanamori et al., 2020). For a given magnitude, σ_a is log-normal distributed with a significant log-normal standard deviation (0.41 in log10 units, Baltay et al., 2011). Baltay and Hanks (2014) showed that the mean peak ground acceleration (PGA) and mean peak ground velocity (PGV) at stations close to the faults for $3 < M < 8$ shallow earthquakes in tectonically active regions (Ancheta et al., 2014) can be matched with a point source stochastic procedure and Brune’s spectral model with $\widetilde{\Delta\sigma}$ of 4.64 MPa. It is equivalent to saying that these data can be modeled using Brune ω^{-2} source spectra with an apparent stress σ_a of 1.1 MPa —consistent with the mean σ_a previously reported for global shallow earthquakes. In fact, the mean σ_a maybe more robust than

$\widetilde{\Delta\sigma}$ because $\widetilde{\Delta\sigma}$ is model-dependent. Ji and Archuleta (2020) found that the data studied by Baltay and Hanks (2014) can be well explained using a double-corner frequency (DCF) source spectrum. While the stress parameter of these DCF models cannot be properly defined, the predicted apparent stress σ_a is 0.73 MPa using the self-similar model JA19. If one uses the non-self-similar JA19_2S model, the synthetic σ_a varies slightly from 1.6 MPa to 0.73 MPa when the moment magnitude changes from 5.3 to 7.3, with a geometric mean of 1.1 MPa. Ji and Archuleta (2020) also noted that the predicted σ_a of additive DCF spectral model AS00 (for California earthquakes, Atkinson and Silva, 2000) has a similar magnitude dependency as JA19_2S (Ji and Archuleta, 2020). On the other hand, the σ_a of additive DCF spectral model AB95 (for eastern North-California earthquakes, Atkinson and Boore, 1995) is considerably larger, possibly reflecting the tectonic significance.

The stress parameter $\widetilde{\Delta\sigma}$ may not be equal to the average static stress drop $\Delta\sigma_s$ on the fault (Atkinson and Beresnev, 1998). In literature, the apparent stress σ_a was considered as an estimate that is related to dynamic/effective stress drop (Madariaga, 1976; Boatwright, 1984; Ji and Archuleta, 2020). The inequality $\widetilde{\Delta\sigma} > \Delta\sigma_s$ has been noticed during the studies of large California and eastern North America earthquakes (e.g., Hanks and McGuire, 1981; Boore, 1983; Atkinson and Beresnev, 1998). This inequality may on average hold for $M_w > 5$ shallow crustal earthquakes in tectonically active regions. For these earthquakes, the scaling relationship $M \sim \log(A) + 4$, where A is in km^2 , is generally applied (e.g., Leonard, 2010). This scaling relation suggests a $\Delta\sigma_s$ of 3 MPa. By analyzing the results of finite fault slip models, Somerville *et al.* (1999) and Irikura and Miyake (2010) reported a mean $\Delta\sigma_s$ of 2.3 MPa. Both results are smaller than the $\widetilde{\Delta\sigma}$ of 4.64 MPa (Baltay and Hanks, 2014). If $\widetilde{\Delta\sigma}$ of 4.64 MPa is equivalent with $\sigma_a \sim 1.1$ MPa and $\Delta\sigma_s \sim 3.0$ MPa, η_R^A of 0.7 would be suggested. The inequality $\widetilde{\Delta\sigma} > \Delta\sigma_s$ of shallow crustal earthquakes, which still needs further confirmation, then suggests that the mean η_R^A of shallow crustal earthquakes is $\sim 50\%$ larger than that of Brune's model (~ 0.466 , Table 1). Shallow crustal earthquakes radiate, on average, more seismic energy than what is predicted by Brune's model, Madariaga's model, and K&S's model.

However, this interpretation has caveats. First, $\widetilde{\Delta\sigma}$ is constrained by the seismic radiation within a limited frequency band. The strong ground motion parameters such as PGA and PGV, which are used to constrain $\widetilde{\Delta\sigma}$ (Hanks and McGuire, 1981; Boore, 1983; Baltay and Hanks, 2014), are sensitive to band-limited seismic signals. Because of path attenuation, seismic signals with frequency above 8-10 Hz have negligible contributions to the strong ground motion parameters (Hanks and McGuire, 1981; Anderson and Hough, 1984; Baltay and Hanks, 2014). Second, Atkinson and Silva (2000) pointed out that a slight decrease of $\widetilde{\Delta\sigma}$ with magnitude for M_w 5.0-7.5 earthquakes was observed (Atkinson and Silva, 1997); this can be interpreted as a finite fault effect (Atkinson and Silva, 1997) or a consequence of the non-self-similar scaling fault length relation (Ji and Archuleta, 2022). Third, the value of $\widetilde{\Delta\sigma}$ is related to the assumptions about site effects, geometric spreading, and earth attenuation (Boore, 1983; Baltay and Hanks, 2014), which were used in earthquake seismology might not be the same as what were used in earthquake seismology.

Because of the importance of $\widetilde{\Delta\sigma}$ in engineering seismology and σ_a in earthquake seismology, systematic investigations of $\Delta\sigma_{ER}^B$ (energy based Brune's stress drop, Ji *et al.*, 2022) and $\widetilde{\Delta\sigma}$ remain a high priority.

III Publications

Ji, C., and R. J. Archuleta (2022). A Source Physics Interpretation of Nonsimilar Double-Corner-Frequency Source Spectral Model JA19_2S, *Seismol. Res. Lett.*, **93**, no. 2A, 777-786. doi:10.1785/0220210098.

Ji, C., R. J. Archuleta, and Y. Wang (2022). Variability of Spectral Estimates of Stress Drop Reconciled by Radiated Energy, *Bull. Seismol. Soc. Am.*, **112**, no. 4, 1871-1885. doi:10.1785/0120210321.

Reference

Ancheta, T. D., R. B. Darragh, J. P. Stewart, E. Seyhan, W. J. Silva, B. S. J. Chiou, K. E. Wooddell, R. W. Graves, A. R. Kottke, D. M. Boore, T. Kishida, and J. L. Donahue (2014). NGA-West2 Database, *Earthquake Spectra*, **30**, no. 3, 989-1005. doi:10.1193/070913eqs197m.

Anderson, J. G., and S. E. Hough (1984). A Model for the Shape of the Fourier Amplitude Spectrum of Acceleration at High-Frequencies, *Bull. Seismol. Soc. Am.*, **74**, no. 5, 1969-1993.

Andrews, D. J. (1986). Objective Determination of Source Parameters and Similarity of Earthquakes of Different Size, in *Earthquake Source Mechanics (Geophysical Monograph Series)* S. Das, J. Boatwright and C. H. Scholz (Editors), American Geophysical Union, 259-267.

Atkinson, G. M., and D. M. Boore (1995). Ground-Motion Relations for Eastern North-America, *Bull. Seismol. Soc. Am.*, **85**, no. 1, 17-30.

Atkinson, G. M., and W. Silva (1997). An empirical study of earthquake source spectra for California earthquakes, *Bull. Seismol. Soc. Am.*, **87**, no. 1, 97-113.

Atkinson, G. M., and I. Beresnev (1998). Don't call it stress drop, *Seismol. Res. Lett.*, **68**, no. 1, 3-4.

Atkinson, G. M., and W. Silva (2000). Stochastic modeling of California ground motions, *Bull. Seismol. Soc. Am.*, **90**, no. 2, 255-274. doi:10.1785/0119990064.

Baltay, A., S. S. Ide, G. Prieto, and G. Beroza (2011). Variability in earthquake stress drop and apparent stress, *Geophys. Res. Lett.*, **38**. doi:10.1029/2011gl046698.

Baltay, A., S., and T. C. Hanks (2014). Understanding the Magnitude Dependence of PGA and PGV in NGA-West 2 Data, *32*, **104**, no. 6, 2851-2865.

Boatwright, J. (1984). Seismic Estimates of Stress Release, *J. Geophys. Res.*, **89**, no. Nb8, 6961-6968. doi:DOI 10.1029/JB089iB08p06961.

Boore, D. (1983). Stochastic Simulation of High-Frequency Ground Motions Based on Seismological Models of the Radiated Spectra, *Bull. Seismol. Soc. Am.*, **73**, no. 6, 1865-1894.

Boore, D., M., C. Di Alessandro, and N. A. Abrahamson (2014). A Generalization of the Double-Corner-Frequency Source Spectral Model and Its Use in the SCEC BBP Validation Exercise, *Bull. Seismol. Soc. Am.*, **104**, no. 5, 2387-2398. doi:10.1785/0120140138.

Boore, D. M. (2003). Simulation of ground motion using the stochastic method, *Pure Appl. Geophys.*, **160**, no. 3-4, 635-676. doi:10.1007/Pl00012553.

Brune, J. N. (1970). Tectonic Stress and Spectra of Seismic Shear Waves from Earthquakes, *J. Geophys. Res.*, **75**, no. 26, 4997-5009.

Convers, J. A., and A. V. Newman (2011). Global evaluation of large earthquake energy from 1997 through mid-2010, *J. Geophys. Res.*, **116**. doi:10.1029/2010jb007928.

Crempien, J. G. F., and R. J. Archuleta (2015). UCSB Method for Simulation of Broadband Ground Motion from Kinematic Earthquake Sources, *Seismol. Res. Lett.*, **86**, no. 1, 61-67. doi:10.1785/0220140103.

Graves, R. W., and A. Pitarka (2010). Broadband Ground-Motion Simulation Using a Hybrid Approach, *Bull. Seismol. Soc. Am.*, **100**, no. 5a, 2095-2123. doi:10.1785/0120100057.

Hanks, T. C., and H. Kanamori (1979). Moment Magnitude Scale, *J. Geophys. Res.*, **84**, no. Nb5, 2348-2350. doi:10.1029/JB084iB05p02348.

Hanks, T. C., and R. K. McGuire (1981). The Character of High-Frequency Strong Ground Motion, *Bull. Seismol. Soc. Am.*, **71**, no. 6, 2071-2095.

Husseini, M. I., and M. J. Randall (1976). Rupture Velocity and Radiation Efficiency, *Bull. Seismol. Soc. Am.*, **66**, no. 4, 1173-1187.

Ide, S., and G. C. Beroza (2001). Does apparent stress vary with earthquake size?, *Geophys. Res. Lett.*, **28**, no. 17, 3349-3352. doi:10.1029/2001gl013106.

Ide, S., G. C. Beroza, S. G. Prejean, and W. L. Ellsworth (2003). Apparent break in earthquake scaling due to path and site effects on deep borehole recordings, *Journal of Geophysical Research: Solid Earth*, **108**, no. B5. doi:10.1029/2001jb001617.

Irikura, K., and H. Miyake (2010). Recipe for Predicting Strong Ground Motion from Crustal Earthquake Scenarios, *Pure Appl. Geophys.*, **168**, no. 1-2, 85-104. doi:10.1007/s00024-010-0150-9.

Ji, C., and R. J. Archuleta (2020). Two Empirical Double-Corner-Frequency Source Spectra and Their Physical Implications, *Bulletin of the Seismological Society of America*, 10.1785/0120200238. doi:10.1785/0120200238.

Ji, C., and R. J. Archuleta (2020). Two empirical double-corner frequency source spectra and their physical implications, *Bull. Seismol. Soc. Am.*, 10.1785/0120200238. doi:10.1785/0120200238.

Ji, C., and R. J. Archuleta (2022). A Source Physics Interpretation of Nonself-Similar Double-Corner-Frequency Source Spectral Model JA19_2S, *Seismol. Res. Lett.*, **93**, no. 2A, 777-786. doi:10.1785/0220210098.

Ji, C., R. J. Archuleta, and Y. Wang (2022). Variability of Spectral Estimates of Stress Drop Reconciled by Radiated Energy, *Bull. Seismol. Soc. Am.*, **112**, no. 4, 1871-1885. doi:10.1785/0120210321.

Kanamori, H., Z. E. Ross, and L. Rivera (2020). Estimation of radiated energy using the KiK-net downhole records—old method for modern data, *Geophys. J. Int.*, **221**, no. 2, 1029-1042. doi:10.1093/gji/ggaa040.

Leonard, M. (2010). Earthquake Fault Scaling: Self-Consistent Relating of Rupture Length, Width, Average Displacement, and Moment Release, *Bull. Seismol. Soc. Am.*, **100**, no. 5a, 1971-1988. doi:10.1785/0120090189.

Liu, P. C., R. J. Archuleta, and S. H. Hartzell (2006). Prediction of broadband ground-motion time histories: Hybrid low/high-frequency method with correlated random source parameters, *Bull. Seismol. Soc. Am.*, **96**, no. 6, 2118-2130. doi:10.1785/0120060036.

Madariaga, R. (1976). Dynamics of an Expanding Circular Fault, *Bull. Seismol. Soc. Am.*, **66**, no. 3, 639-666.

Prieto, G. A., P. M. Shearer, F. L. Vernon, and D. Kilb (2004). Earthquake source scaling and self-similarity estimation from stacking P and S spectra, *Journal of Geophysical Research: Solid Earth*, **109**, no. B8. doi:10.1029/2004jb003084.

Schmedes, J., R. J. Archuleta, and D. Lavallee (2013). A kinematic rupture model generator incorporating spatial interdependency of earthquake source parameters, *Geophys. J. Int.*, **192**, no. 3, 1116-1131. doi:10.1093/gji/ggs021.

Shao, G. F., C. Ji, and E. Hauksson (2012). Rupture process and energy budget of the 29 July 2008 M-w 5.4 Chino Hills, California, earthquake, *J. Geophys. Res.*, **117**. doi:10.1029/2011jb008856.

Singh, S. K., and M. Ordaz (1994). Seismic Energy-Release in Mexican Subduction Zone Earthquakes, *Bull. Seismol. Soc. Am.*, **84**, no. 5, 1533-1550.

Somerville, P., K. Irikura, R. Graves, S. Sawada, D. Wald, N. Abrahamson, Y. Iwasaki, T. Kagawa, N. Smith, and A. Kowada (1999). Characterizing Crustal Earthquake Slip Models for the Prediction of Strong Ground Motion, *Seismol. Res. Lett.*, **70**, no. 1, 59-80. doi:10.1785/gssrl.70.1.59.

Venkataraman, A., and H. Kanamori (2004). Observational constraints on the fracture energy of subduction zone earthquakes, *J. Geophys. Res.*, **109**, no. B5. doi:10.1029/2003jb002549.